Published in Journal of Contaminant Hydrology, 74, issues 1-4, 231-252, 2004
which should be used for any reference to this work

Bacteriophage transport through a fining-upwards sedimentary sequence: laboratory experiments and simulation

Raymond Flynn[a,*], Fabien Cornaton[a], Daniel Hunkeler[a], Pierre Rossi[b]

[a] *Hydrogeology Centre, University of Neuchatel, Rue Emile-Argand, 11, CH-2007 Neuchatel, Switzerland*
[b] *Microbiology Laboratory, University of Neuchatel, Emile-Argand, 11, CH-2007 Neuchatel, Switzerland*

Abstract

A column containing four concentric layers of progressively finer-grained glass beads (graded column) was used to study the transport of the bacteriophage T7 in water flowing parallel to layering through a fining-upwards (FU) sedimentary structure. By passing a pulse of T7, and a conservative solute tracer upwards through a column packed with a single bead size (uniform column), the capacity of each bead type to attenuate the bacteriophage was determined. Solute and bacteriophage responses were modelled using an analytical solution to the advection–dispersion equation, with first-order kinetic deposition simulating bacteriophage attenuation. Resulting deposition constants for different flow velocities indicated that filtration theory-determined values differed from experimentally determined values by less than 10%. In contrast, the responses of solute and bacteriophage tracers passing upwards through graded columns could not be reproduced with a single analytical solution. However, a flux-weighted summation of four one-dimensional advective–dispersive analytical terms approximated solute breakthrough curves. The prolonged tailing observed in the resulting curve resembled that typically generated from field-based tracer test data, reflecting the potential importance of textural heterogeneity in the transport of dissolved substances in groundwater. Moreover, bacteriophage deposition terms, determined from filtration theory, reproduced the T7 breakthrough curve once desorption and inactivation on grain surfaces were incorporated. To evaluate the effect of FU sequences on mass transport processes in more detail, bacteriophage passage through sequences resembling those sampled from a FU bed in a fluvioglacial gravel pit were carried out using an analogous approach to that employed in the laboratory. Both solute and bacteriophage breakthrough responses resembled those generated from field-based test data and in the graded column experiments. Comparisons with the results of simulations using averaged hydraulic conductivities show that simulations employing averaged parameters overestimate bacteriophage travel times and underestimate masses recovered and peak concentrations.

Keywords: Groundwater; Bacteriophage; Sedimentary structure; Tracer; Porous aquifer; Heterogeneity

* Corresponding author. Fax: +41-32-718-26-03.
E-mail address: ray.flynn@unine.ch (R. Flynn).

1. Introduction

Groundwater is the principal source of drinking water in many parts of the world (van der Leeden et al., 1990). In order to better understand and protect the quality of this resource, an understanding of the processes controlling contaminant occurrence and migration is necessary. Microorganisms such as viruses, bacteria and protozoa form an important category of pollutants that pose a significant threat to public health due to their occurrence in drinking water. Macler and Merkle (2000) estimate that between 750,000 and 5.9 million waterborne illness associated with microbiologically contaminated groundwater occur in the United States each year. The same authors note that, despite recent research, our understanding of how such contamination occurs in groundwater is far from complete and needs additional investigation. A critical aspect of microbiological contamination of groundwater relates to how microorganisms manage to reach water sources. Robertson and Edberg (1997) noted that many microorganisms have been shown to migrate considerable distances in various groundwater environments, demonstrating that the problem of microorganism occurrence in aquifers is not necessarily restricted to the zone immediately surrounding water supply wells.

Comparative tracer testing provides a means of studying microorganism transport in water by comparing their responses to that of a simultaneously injected conservative solute tracer. In recent years, a large number of studies have investigated the transport and attenuation of microorganisms in this way. These studies have included investigations into transport and attenuation of the major microbiological groups that pose significant threat to public health, including protozoa, (e.g. Harter et al. (2000)), bacteria, (e.g. Bolster et al. (1999)) and viruses (e.g. Redman et al. (2001)).

Tracer investigations may be laboratory based and may be carried out even down to the level of individual pores (Lawrence and Hendry, 1996). Laboratory-based studies have the benefit of permitting conditions to be closely controlled and the fundamental processes influencing microorganism transport and attenuation to be identified. At the other end of the scale, field-based investigations allow in-situ studies of microorganism transport and attenuation to be carried out, and the relative importance of different attenuation mechanisms identified in the laboratory to be assessed in aquifers (e.g. Schijven et al., 2000).

Many workers have noted that tracer responses with time (breakthrough curves) observed on different scales may not be consistent with one another (Harvey and Garabedian, 1991; Bales et al., 1995; Schijven et al., 2002). These differences are often attributed to heterogeneity. The influence of heterogeneity can be compositional, due to variations in the surface composition, as shown for example in laboratory-based studies

completed by Johnson et al. (1996). Heterogeneity may also be textural, due to differences in grain size. Column studies by Saiers and Hornberger (1996) noted that simple heterogeneities, such as a tubule of coarse-grained sand set in a fine-grained matrix, could significantly alter tracer breakthrough curves. Moreover, column studies by Martin et al. (1992) demonstrated the appropriateness of filtration theories predicting bacterial removal in porous media for various grain sizes.

On the field scale, many differences in solute and microorganism breakthrough curves have been attributed to geological heterogenity in a variety of depositional environments ranging from relatively uniform fine sands (Schijven et al., 1999) to very coarse montane alluvial gravels (Woessner et al., 1998). Many of these tests have used bacteriophage (bacterial viruses or phage) as viral surrogates because of the technical and logistical complications of working with pathogenic virus types. Recent tracer tests carried out at the Kappelen porous medium test site (Kennedy et al., 2001a), in Canton Bern, Switzerland have a demonstrated striking difference in bacteriophage and solute tracer responses during comparative tracer tests in a fluvioglacial sand and gravel aquifer (Fig. 1). The breakthrough curves in Fig. 1 show that as the solute and bacteriophage tracers arrived at an observation well, the rising limb of the bacteriophage breakthrough curve followed that of the conservative solute before truncating and rapidly declining, while the solute concentration continued to rise. Following a steep decline, a point of inflection on the bacteriophage breakthrough curve was reached, after which concentrations declined much more gradually. The net result of this process was that peak virus concentrations were observed earlier than peak solute concentrations. Furthermore, total bacteriophage recovery was less than that of the conservative solute tracer over the monitoring period. It is noteworthy that data analysis using solutions to the advection–dispersion equation has been incapable of satisfactorily reproducing either of the breakthrough curves observed in this test.

Despite the extensive work completed to date, studies that investigate the effects of intermediate-scale structures (between column-scale studies and field-scale investigations) on solute and particle tracer transport, are less common (e.g. Silliman, 2000). Indeed, studies at this scale may be necessary if the differences in tracer response between column-scale studies and field investigations are to be resolved. Many sedimentary structures fall into the category of intermediate size structures, including phenomena such as cross-bedding, coarsening-upward sequences and fining-upward sequences in sediments, where variations in grain size/mineralogy occur within individual beds. Reading (1986) observed that such phenomena are widespread in consolidated and unconsolidated sediments in a wide variety of depositional environments. Moreover, Dieulin (1980) noted the importance of such units on the breakthrough of conservative solutes in alluvial deposits.

This study investigated the transport of the bacteriophage T7 and a conservative solute tracer through a fining-upward (FU) sequence of sediments. Tracer responses were investigated using a column packed with concentric layers of progressively coarser-grained glass beads (graded column). The bacteriophage attenuation characteristics of each bead type used were determined in a series of complimentary tests where the tracers were passed through columns packed with a single bead size (uniform columns) and the resulting responses numerically modelled. Variations in flow velocity through the uniform columns permitted the applicability of conventional filtration theory to the experimental system to be validated and subsequently employed to simulate bacteriophage response in the graded

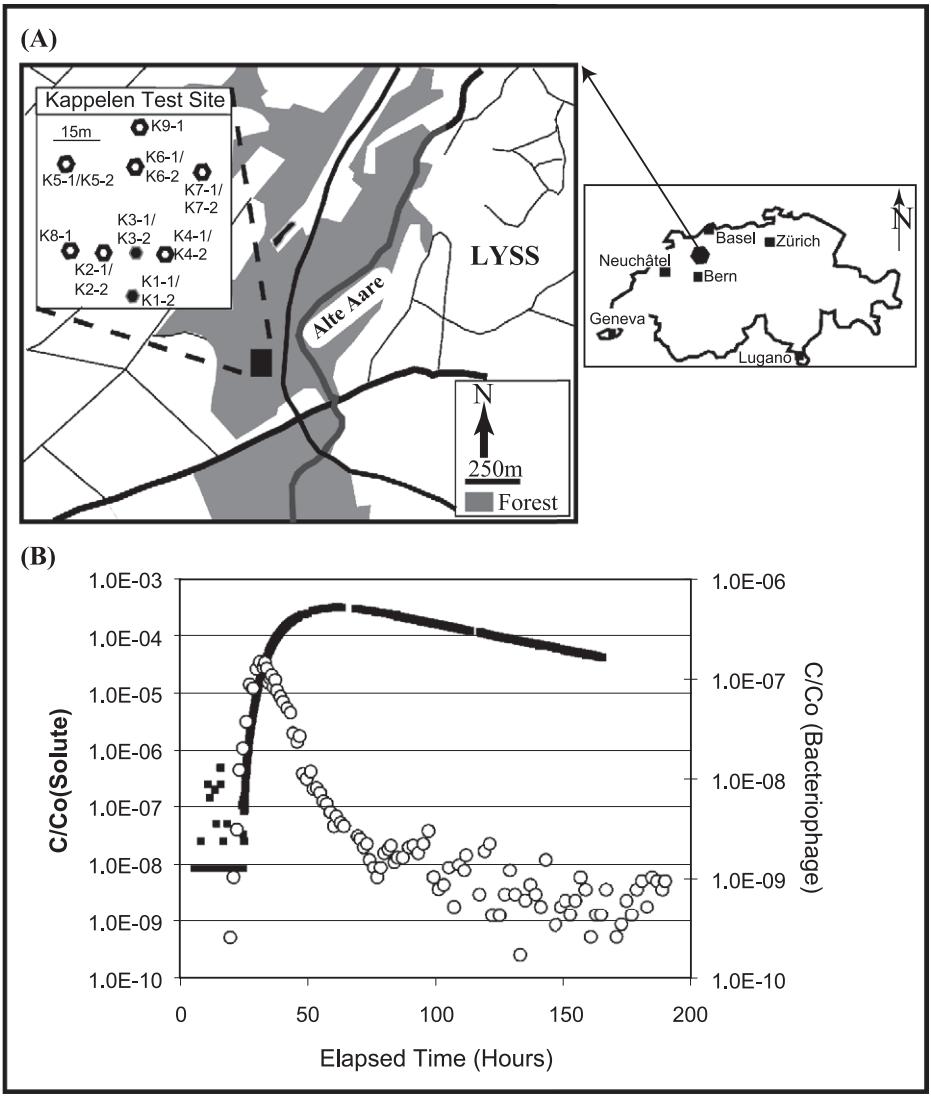

Fig. 1. (A) Location map of Kappelen Porous Medium Test Site, Canton Bern, Switzerland with inlay showing monitoring well locations. (Monitoring well K3-2 and injection well K1-2 highlighted in black.) (B) Solute/ bacteriophage breakthrough curves at K3-2 for tracer test completed July 2001. *Note solute and bacteriophage curves plotted on different scales to highlight difference in tracer response.

column experiments. The modelling approach employed in the graded column experiment simulations was subsequently used to simulate tracer responses in a natural FU sequence reconstructed using granulometric data derived from a graded bed of fluvioglacial gravel. The simulations investigated the influence of attenuation capacity and grain size on solute and bacteriophage response and compared results to those observed in field-based studies.

2. Materials and methods

2.1. Glass beads

All column experiments used spherical soda lime glass beads (Potters Industries, Germany) as the porous matrix for column experiments. The experiments investigated the attenuation capacity of four different bead sizes measuring 63 mm, 125, 250 and 500 μm in diameter. In order to remove impurities from the glass surface before starting the experiments, the beads were soaked in 0.1 N NaOH for 45 min, before rinsing in deionised water and soaking in 0.1 N HNO_3 for 45 min. This process was followed by thoroughly rinsing the beads in deionised water and drying at 60 °C. Furthermore, in order to minimize potential cross-contamination between experiments, the beads were placed in a sieve with a finer mesh size than the beads and thoroughly washed in deionised water prior to drying for 20 h at 60 °C following each experiment.

2.2. Synthetic freshwater/solute tracer

A synthetic freshwater, consisting of precise quantities of selected salts dissolved in Nanopure© (Barnsted, Van Nuys, USA) water was prepared according to Moore et al. (1982). Two millilitres per litre of 0.1 M Potassium hydrogenophtalate ($C_8H_5KO_4$) (Merck) buffer was added to the water and the pH of the system adjusted to 4.6 with 1 N HCl.

The resulting synthetic freshwater acted as the tracer solvent/suspending liquid and flush water for the column experiments. A 100-ppb (0.1 mg l^{-1}) solution of sodium fluorescein (Uranin, Fluka, Buchs, Switzerland) acted as the solute tracer. Kass (1997) summarised studies indicating that although sodium fluorescein (fluorescein) is pH sensitive and degrades in strong light, it undergoes little to no interaction with inorganic materials and was thus assumed to act conservatively during the column tests.

2.3. Bacteriophage tracer

Bacteriophage are non-pathogenic colloid-sized particles that infect specific species of bacteria. Preliminary multiple phage experiments carried out in the wider framework of this study using the coliphages MS-2 and T7, in conjunction with the marine phage types H6/1 and H40/1, demonstrated that significant amounts T7 were attenuated by glass beads between pH 4 and pH 5. In contrast, the other phage types were not significantly attenuated. Consequently, T7 was selected to study phage attenuation in the above pH range, rather than modifying hydrochemical conditions to permit attenuation of other phage types to be studied (e.g. by increased ionic strength and/or lower pH), yet risking excessive inactivation of phage in suspension. T7's capsid (head) measures 17 nm in diameter and it has a 43-nm-long tail. The phage belongs to the *Podoviridae* family (morphotype C1) and is hosted by the bacterium *Escherichia coli B*. Although T7 has a long tail, unlike most pathogenic viruses, this aspect of its morphology is not suspected to play an important role in its attenuation. Studies of the tailed phage λ, by Penrod et al. (1996) found strong evidence that phage attachment was determined primarily by capsid

surface charge, and that the tail contributes relatively little to the overall charge. By analogy, the behaviour of T7 was similarly not suspected to be strongly influenced by the presence of its tail. It is therefore suspected of behaving similarly in groundwater to viruses lacking tails, such as many pathogenic virus types.

Zeta potential measurements made using a Zeta Master (Malvern Instruments, Malvern, UK), within the framework of this study, showed that T7 has a zeta-potential in synthetic freshwater at pH 6.2 of between -8 and -16 mV. Measurements made at pH 8.5 determined the phages zeta potential to be -29 mV. Similarly, hydrophobicity measurements made using a contact angle microscope showed this phage type to be slightly hydrophobic (Contact angle: 89° to 92°).

Prior to starting the experiments, T7 production was carried out on Petri dishes using Luvia Bertani agar (LB) with a double agar layer technique. The confluent lysis on the surface of the double agar layer of the petri dishes plates was scrapped, mixed in a small volume of saline buffer (0.9 g l^{-1} NaCl) and centrifuged (15 min, 12,000 × g) to remove bacterial cells and agar debris. The supernatant acted as the virus stock (source concentrate) and was stored at 4 °C to minimize viral inactivation (loss of virulence) throughout the whole set of experiments.

At the start of an experiment, phage stock was diluted in saline buffer and 9 μl added to the source reservoir containing the solute tracer and mixed using a Teflon-coated magnetic stirrer. Source samples collected from the tracer reservoir immediately after mixing, and at regular intervals until the end of the experiment, permitted source concentration variation with time to be determined, and thus viral inactivation rates in the source reservoir could be evaluated.

Phage counts were assayed using an optimized double agar layer (Rossi and Kass, 1997) on the LB medium. Rossi and Aragno (1999) found the detection limit using this method to be less than one plaque-forming unit per ml (Pfu ml^{-1}). The results of duplicate analyses for each sample were quantified the day after cultivation, by direct counting. Concentration differences between duplicate analyses for a sample were typically within 25% of one another.

2.4. Column experiment procedure

Two types of column experiments were carried out in order to characterise phage flow and transport in a FU sedimentary structure. Experiments investigating phage transport through a uniform matrix using a single bead size employed a 25-cm-long, 1.9-cm internal diameter borosilicate glass column (uniform column). Graded column experiments investigated flow in a column containing concentric layers of differently sized beads that became progressively finer-grained toward the centre, employing a 30-cm-long, 5.4-cm internal diameter perspex column.

In uniform column experiments, the column was packed in 1-cm increments by pouring a single bead size into degassed synthetic freshwater less than 3 cm deep. Tapping of the matrix surface with a solid glass rod reduced the possibilities of grain bridging and the development of preferential flow paths.

An analogous packing procedure was followed for the graded column experiments. The four grain-size fractions, as used in the uniform column experiments, were emplaced into

separate thin-walled (ca. 0.2 mm thick) hollow cylinders, set concentrically around one another and resting on a 1-cm-thick filter layer of uniform 500-μm diameter beads (Fig. 2). This graded column system set the finest size fraction in the centre of the column, whereas progressively coarser fractions were placed further towards the column walls. The column was packed in this manner to reproduce a progressively finer-grained structure. The cylinder diameters were arranged in such a way that the cross-sectional area of each grain-size fraction in the column was equal. Once the cylinders were packed, the thin cylinder walls were slowly withdrawn from the column. Upon complete withdrawal, an additional 2-cm layer of uniform 500-μm diameter beads were place on top of the column, prior to sealing the saturated fully packed column.

During uniform column and graded column experiments, a peristaltic pump (Ismatec IP-15, Glattbrugg, Switzerland), connected to the column by 4-mm OD silicone tubing, pumped water/tracer upwards through the column at a constant rate. At least 10 pore volumes of tracer-free synthetic freshwater circulated through the system to ensure chemical equilibration prior to starting tracer injection. Influent and effluent pH and electrical conductivity were regularly monitored to ensure that the chemistry of the waters

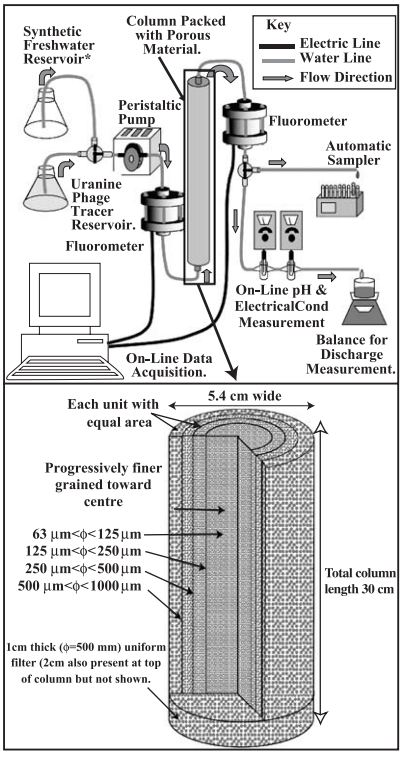

Fig. 2. Schematic illustration of column apparatus used during bacteriophage tracer test experiments with detail of graded column apparatus. Column used for (uniform) experiments with single bead size: 25 cm long × 1.9 cm in diameter.

at the column entrance and exit points did not differ significantly from each other. All experiments were completed at between 21 and 24 °C.

Both graded column experiments and uniform column experiments were repeated at least twice for each grain-size fraction to provide an indication of the variation in results between experiments due to packing. Following the graded column tests, the various grain-size fractions used were separated by wet sieving using standard sieve sizes (DIN. ISO 3310/1), and washed with de-ionised water. The separated fractions were dried at 60 °C for 20 h prior to re-use.

Three pore volumes of solute/phage tracer were injected during uniform column experiments. This approach permitted the principal virus attenuation characteristics to be investigated. The prolonged injection of a constant tracer concentration allowed the possibility that there were a limited number of deposition sites in the column matrix to be determined. Were this to be the case, a gradual rise in phage concentration would be observed in the column effluent, relative to the solute tracer concentrations. The experiments were carried out at constant flow rates of approximately 4.2 and 1.6 ml min^{-1} for the three coarsest grain-size fractions in order to evaluate the influence of variable flow velocity on T7s attenuation. Experiments in the finest grain-size fraction were only carried out at the lower flow rate since it was feared that the higher flow rate might generate excessive hydraulic gradients resulting in a rupturing of the matrix and the development of preferential flow paths.

Since tracers are typically injected in short pulses during field-based experiments, and one of the principal objectives of graded column experiments was to attempt to reproduce conditions observed at the field scale, approximately 0.3 pore volumes of tracer were injected into the column. Kretzschmar et al. (1997) note that short pulse experiments of this type provide an excellent agreement with step pulse experiments, where more than one pore volume is injected, once first-order deposition is the dominant attenuation process.

On-line fluorometers monitored solute tracer concentrations in column influent and effluent water at 10-s intervals (corresponding to 0.01–0.03 pore volumes, depending on flow rate) and could detect fluorescein at concentrations as low as 0.1 ppb (Schnegg and Bossy, 2001). An automatic sampler continuously collected column effluent samples for virus analysis at 0.2 pore volume intervals. Furthermore, regular on-line measurements of pH and conductivity continued to ensure that hydrochemical conditions remained constant during all experiments. Fig. 2 summarises details of the experimental setup and design.

2.5. Natural granular media

In order to evaluate grain size and subsequent hydraulic conductivity variation in a sedimentary structure, samples were collected from a bed containing a FU sequence of sand and gravel for granulometric analysis. The sampling location was a recently exposed face in the Walperswil fluvioglacial gravel pit, (Walperswil, Canton Bern, Switzerland—Fig. 3A), approximately 5 km northwest of the Kappelen Test Site. Discrete samples were taken from freshly excavated deposits in 2- to 5-cm-thick intervals ranging from the erosive base of the bed to the top of the ca. 30–35-cm-thick FU sequence. Clean stainless steel plates set above and below each sample interval isolated the deposits to be excavated from adjacent samples, while preventing finer-grain-sized fractions from being lost during

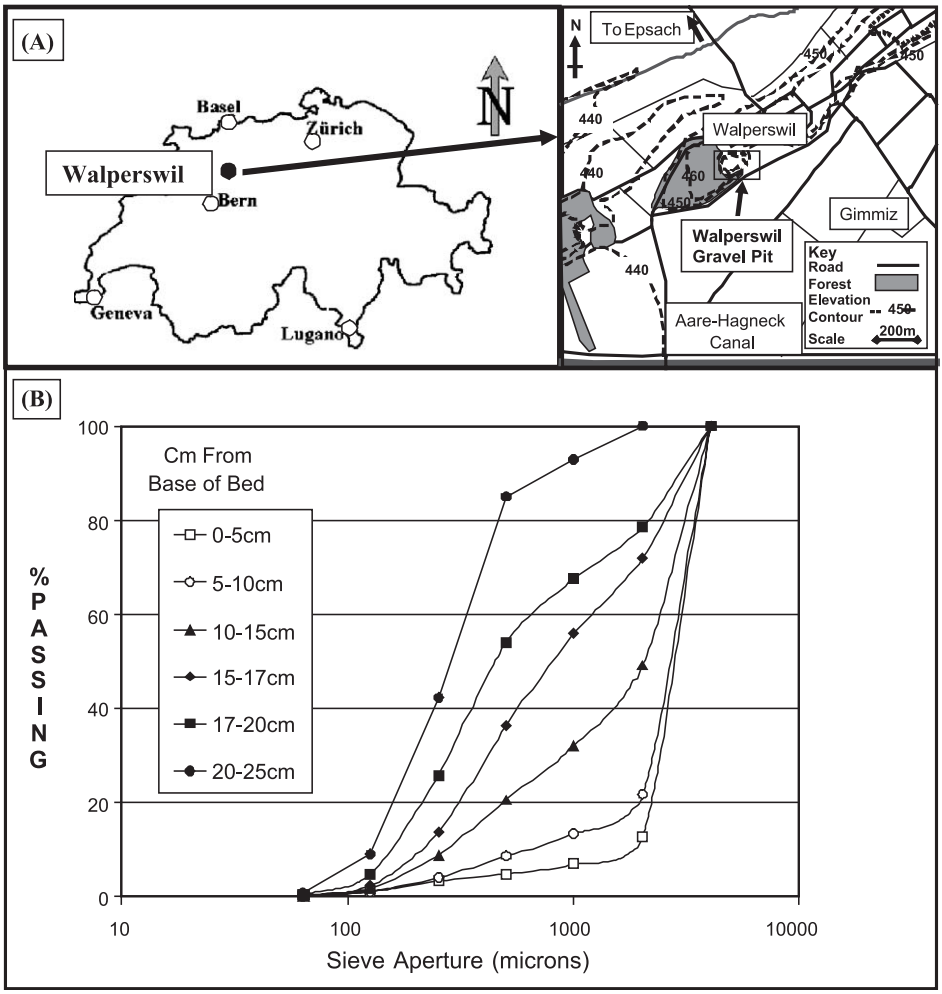

Fig. 3. (A) Sampling location map for Walperswil gravels. (B) Representative grain-size distribution curves for samples collected from a section through a fining-upward sequence.

sampling. In this way, a total of 21 samples were collected from three different sections in the bed. All three sections were located within one m of one another.

Visual examination of field samples revealed them to be dominated by subrounded to well rounded gravel with a subordinate proportion of sand, which became more predominant toward the top of the bed. Furthermore, field-based inspection indicated that carbonates and framework silicates (quartz and feldspars) dominated sample mineralogy.

The sand and gravel samples were subdivided into differing grain-size fractions by agitated wet sieving using standard sieve sizes (DIN. ISO 3310/1) and subsequently oven dried at 40 °C overnight, before weighing. (Fig. 3B presents the grading curves for six samples collected from one of the sections).

3. Numerical interpretation

Virus transport characteristics were evaluated using the advection–dispersion equation, coupled to kinetic parameters derived from classical filtration theory. The fundamental equations governing the transport processes are given by Bolster et al. (1999). These equations have been modified to account for viral inactivation on solid surfaces and suspended in liquid as follows:

$$\frac{\partial C}{\partial t} + \frac{\rho_b}{\theta}\frac{\partial S}{\partial t} = D_l \frac{\partial^2 C}{\partial x^2} - v\frac{\partial C}{\partial x} - \mu_l C - \mu_s \frac{\rho_b}{\theta} S \tag{1}$$

$$\frac{\rho_b}{\theta}\frac{\partial S}{\partial t} = k_c C - k_d \frac{\rho_b}{\theta} S - \mu_s \frac{\rho_b}{\theta} S \tag{2}$$

where C is the concentration of T7 in the liquid (M L^{-3}); S is the adsorbed phage concentration (M L^{-3}); t is time (T); x is distance from the injection point (L); D_L is the (longitudinal) dispersion coefficient (L^2 T^{-1}); v is the advective water velocity (L T^{-1}); ρ_b is the dry bulk density θ is the porosity (–); μ_s and μ_l are inactivation rates of T7 adsorbed onto solid surfaces and in liquid (T^{-1}); k_d is the detachment rate constant (T^{-1}) and k_c is the deposition constant (T^{-1}). Eqs. (1) and (2) were solved in Laplace space for a time-dependent Dirichlet-type boundary condition before being returned to the time domain by numerical inversion using the method of De Hoog et al. (1982).

According to filtration theory, k_c may be determined as follows (Tien and Payatakes, 1979):

$$k = \frac{3(1-\theta)}{2d_c}\eta\alpha v \tag{3}$$

where d_c is the matrix diameter, α is the collision efficiency (–) and η is the single collector efficiency (–). Yao et al. (1971) define the collision efficiency as the probability of attachment resulting from a collision between a particle and a solid surface. Kretzschmar et al. (1999) note that α reflects the attractive properties largely resulting from solution and surface chemistry.

In contrast, the single collector efficiency is strongly dependent on physical parameters of the system including surface area accessible for deposition, pore structure, flow velocity, particle density and particle size. Given T7s small size, η can be calculated using a modification of Rajagopalan and Tien's (1976) equation developed by Penrod et al. (1996):

$$\eta = 4A_s^{\frac{1}{3}} N_{Pe}^{-\frac{2}{3}} \tag{4}$$

where

$$A_s = \frac{2(1-\gamma^5)}{(2-3\gamma+3\gamma^5-2\gamma^6)} \qquad \text{where } \gamma = (1-\theta)^{1/3} \tag{5}$$

$$N_{Pe} = \frac{3\pi\mu d_p d_c q}{kT} \tag{6}$$

where d_p is the particle diameter (1.7×10^{-8} m); μ is the fluid viscosity (9.3×10^{-4} Pa s); q is the specific discharge (m s^{-1}); k is the Boltzman constant (1.38048×10^{-23} J K^{-1}); T is the temperature (295 K).

In both uniform and graded column experiments, T7s transport characteristics were characterised using the solution of Eqs. (1) and (2). Best-fit deposition constants for each size fraction of beads were established from uniform column data by determining the minimum of the residuals between observed and simulated concentrations using the least-squares method. By applying values of η calculated from the filtration theory, based on known porosities and matrix diameters, and using the values of k_c for T7 derived from the solution to Eqs. (1) and (2), α could be calculated using Eq. (3). This parameter could then be used with hydrodynamic data and grain diameter/porosity data to determine phage deposition constants under differing flow regimes in the graded column experiments.

A numerical solute transport model suggested that little lateral exchange occurs over short distances in the graded system. Consequently, it was assumed reasonable to simulate the mass transport regime in the graded column by the superimposition of four one-dimensional analytical terms, taken to represent mass transport through the four different grain-size units. The four units have different advective velocities and dispersion coefficients which generate different individual breakthrough curves. These curves are subsequently added to yield a composite tracer response. Maloszewski (1992) provides a detailed description of this method. Advective velocity and dispersion coefficient were determined by fitting the fluorescein breakthrough curve using the solution to Eq. (1), ensuring that the total simulated outflow corresponded to that observed during the experiment. Using the α values calculated in the uniform column experiments, deposition constants could be calculated for each layer in the graded column using Eqs. (3) and (4) while accounting for different flow velocities, determined from the fluorescein breakthrough curve. Overall bacteriophage breakthrough curves could thus be reconstructed using the flux-weighted average of the four analytical solutions.

3.1. Analytical model—gravel deposits

The hydraulic conductivity of the various intervals sampled in the Walperswil gravels was estimated using the Kozeny–Carman equation (Bear, 1972) with a 5% variation in porosity around a typical value of 30% for gravels (Freeze and Cherry, 1979). The equation relates hydraulic conductivity to grain size as follows:

$$K = \left(\frac{\rho_f g}{\mu}\right)\left(\frac{\theta^3}{(1-\theta^2)}\right)\left(\frac{d_{10}}{180}\right) \tag{7}$$

where d_{10} is the finest 10% retained during sieving, and is regarded as the representative grain diameter in controlling hydraulic conductivity. Martin et al. (1996) demonstrated that the d_{10} diameter is also most appropriate for describing microorganism transport in porous media. Hydraulic conductivites calculated using Eq. (7) were plotted with distance from

the base of the bed and fitted to a best-fit function to determine magnitude of hydraulic conductivity variation with depth in the FU sequence.

Based on the results of the granulometric analyses, solute and bacteriophage transport were simulated through a bed with a similar hydraulic conductivity profile, i.e. hydraulic conductivity varying by a similar magnitude within a 50-cm-thick bed. The bed was discretised into eight 6.25-cm-thick unimodal grain-size units of uniform hydraulic conductivity, and a uniform hydraulic gradient applied across a 50-cm length of the bed. Simulations proceeded in an analogous manner to those in the graded column experiments, i.e. by using the analytical equation summation for simulating breakthrough curves. Deposition constants were calculated using Eqs. (3) and (4) assuming uniform collision efficiency for the entire sequence. Detachment and inactivation constants were kept at approximately the same ratio as those used in reproducing the graded column breakthrough curves. The dispersion coefficient was calculated assuming a constant dispersivity of 1.25 cm. This value resembles that calculated from dispersion coefficient values for the finer-grained beds in graded column experiments.

Simulations were carried out for two different beds with coarser and finer grain sizes to investigate the effect of grain size on phage breakthrough ($\varnothing = 10$ mm to $\varnothing = 1.33$ mm and $\varnothing = 1$ mm to $\varnothing = 0.133$ mm, respectively). The resulting hydraulic conductivities varied over the same order of magnitude as those observed in the Walperswil Gravel samples. The hydraulic gradient was adjusted in each case to ensure equal flow velocities across both beds. Collision efficiencies were 0.3 for the coarser-grained bed and 0.1 for the finer-grained unit. Preliminary simulations in the fine-grained bed, using $\alpha = 0.3$, demonstrated that over 99.9% of viruses recovered were derived from the coarsest grained bed. For this reason, a lower collision efficiency was selected.

The results of these simulations were compared with solute and phage breakthrough curves obtained when averaged grain sizes and hydraulic conductivities were used instead of the coarse-grained FU sequence, assuming equal collision efficiencies.

4. Results

4.1. Uniform column tests

Fig. 4 presents representative breakthrough curves for fluorescein and T7 obtained from the uniform column tests for each bead size. In each size fraction, substantial attenuation of T7 occurred, with the second-smallest sized bead size having the lowest recovery. In all experiments, T7 concentrations reached a plateau suggesting that deposition sites were not a limiting factor in the attenuation process. Significant tailing in the column injection signal prevented accurate assessment of T7 release constants with the analytical approach employed. This is a result of dispersion associated with a difference in diameter between the injection line and the on-line fluorometer measurement cell, resulting in irregular mixing in the cell, rather than pure piston flow. Despite this complication, the data permit deposition constants to be calculated, if the detachment term is assumed negligible in comparison to the adsorption term.

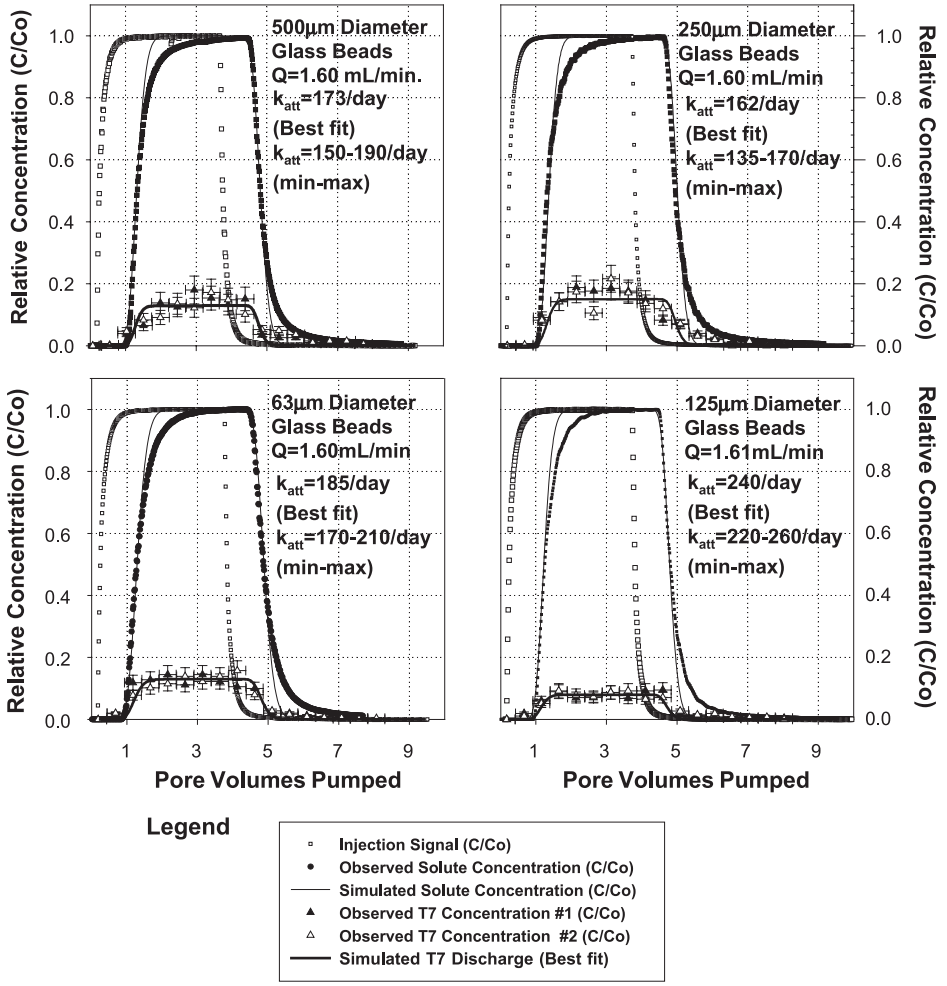

Fig. 4. Representative uniform column breakthrough curves for the four bead sizes investigated. Observed relative concentrations represented as points and simulated breakthrough curves represented as lines. Temporal resolution of T7 data is ± 0.2 pore volumes. Bacteriophage relative concentration error bars $\pm 25\%$ of observed concentration.

It is noteworthy that the range of deposition constants varied within each grain-size fraction. However, once differences in flow velocity and specific flux were accounted for with Eqs. (3)–(6), calculated collision efficiencies for different discharge rates fall into the same range (Table 1) and deposition constants differ from experimentally determined values by less than 10%. This result indicates that the filtration theory is an appropriate means of evaluating T7 deposition constants at different discharge rates in the porous media studied.

Bacteriophage analyses of samples collected from the tracer reservoir during all experiments (uniform column and graded column) indicated that inactivation of

Table 1
Model parameters used to simulate results of uniform (single bead size) column experiments

Experiment	Diameter (μm)	Flow rate (ml min^{-1})	Velocity (m day^{-1})	Dispersion coefficient (m^2 day^{-1})	k_c (day^{-1})	Collision efficiency (−)	Effect. porosity (−)
500 μm #1	500	4.40	60	0.08	235	4.1e − 02	0.37
500 μm #2	500	1.60	21	0.04	173	4.7e − 02	0.39
500 μm #3	500	1.60	21	0.04	152	4.1e − 02	0.39
500 μm #4	500	4.15	55	0.08	238	4.5e − 02	0.38
250 μm #1	250	4.12	60	0.10	210	1.0e − 02	0.35
250 μm #2	250	4.45	60	0.10	243	1.4e − 02	0.38
250 μm #3	250	1.60	21	0.05	162	1.4e − 02	0.39
125 μm #1	125	4.40	60	0.10	282	4.9e − 03	0.37
125 μm #2	125	1.60	23	0.07	240	5.1e − 03	0.35
63 μm #1	63	1.56	24	0.06	218	1.3e − 03	0.33
63 μm #2	63	1.61	22	0.08	185	1.4e − 03	0.37

bacteriophage in synthetic freshwater was not significant over the duration of the experiments.

4.2. Graded column tests: experimental data

Fig. 5 presents the results Graded Column Test #2, along with mathematical model simulation results. The results are representative of all three graded column experiments and reflect the significant differences in T7 and fluorescein breakthrough curves. It is nonetheless worth noting that the irregular oscillations in fluorescein concentration observed at low concentrations in the later part of the curve vary from one experiment to another and are believed to be associated with irregularities due to column packing.

Both T7 and fluorescein breakthrough curves differ from those generated using uniform single grain-size columns, in that both breakthrough curves are considerably more skewed to the left and display significant tailing, despite almost perfect short pulse injection signals. However, even though fluorescein and T7 first arrivals and peak concentrations correspond in the graded column tests within the margins of error, peak T7 concentrations are substantially lower than those of the solute. Moreover, the fluorescein and T7 tailing parts of respective breakthrough curves differ in their characteristics. That of the bacteriophage curve tends to decline more rapidly before flattening out and declining more slowly than that of the fluorescein. These phenomena bear stronger resemblance to breakthrough curves observed in field-based experiments (Fig. 1) than to those observed in laboratory-based uniform column tests.

The advective velocity and dispersion coefficient data, presented in Table 2, permit the fluorescein breakthrough curve to be reproduced using four flux-weighted superimposed analytical solutions, with a total discharge equivalent to that observed (Fig. 5). Moreover, by using these velocity values, T7s kinetic deposition parameters could be determined for each layer of the column based on collision efficiencies determined from uniform column experiments with Eqs. (3) and (4) (Table 2). The resulting parameters permitted T7

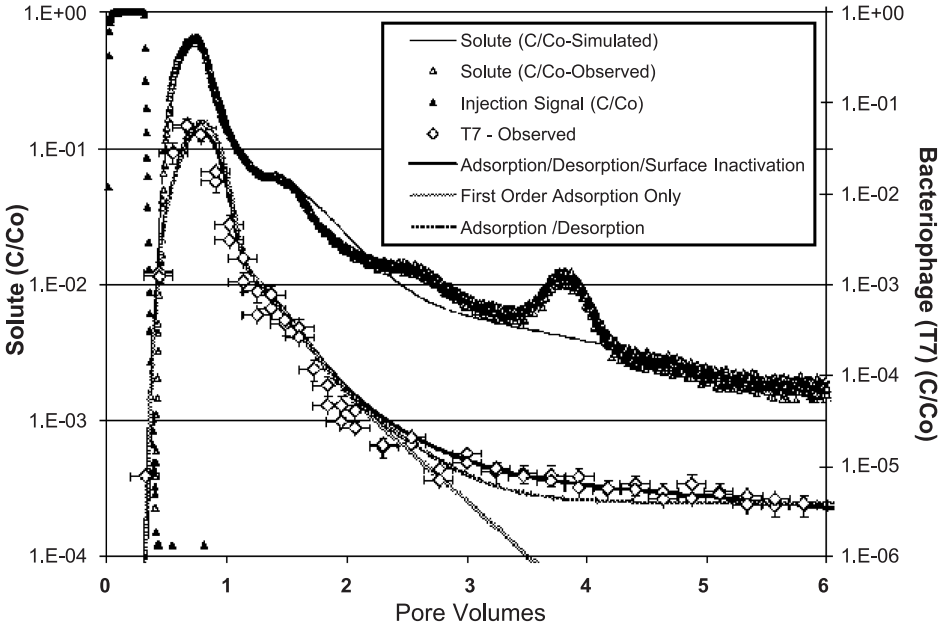

Fig. 5. Logarithmic plot of observed and simulated fluorescein and T7 breakthrough curves for Graded Column Experiment #2. The figure also presents the results of modelling scenarios with first-order adsorption and first-order adsorption/desorption being considered without surface inactivation of T7. Temporal resolution of T7 data is ± 0.2 pore volumes. Bacteriophage relative concentration error bars ± 25% of observed concentration.

breakthrough curves to be generated for all three graded bed simulations. The results of Graded Column test #2, presented in Fig. 5, demonstrate that the calculated first-order deposition parameters provide an excellent fit to the phage breakthrough curve up to

Table 2
Model parameters used to simulate results of graded column experiments

Experiment	Grain diameter (μm)	Flow rate × 1000 (m^3 day^{-1})	Advective velocity (m day^{-1})	Dispersion coefficient (m^2 day^{-1})	Effect porosity (−)	k_c (day^{-1})
Graded bed #1	500	2.117	18.7	0.043	0.19[a]	537
k_d = 0.008 day^{-1}	250	3.175	14.4	0.086	0.44	81
μ_s = 1.0 day^{-1}	125	2.016	8.6	0.086	0.39	130
	63	8.338	3.6	0.086	0.39	84
Graded bed #2	500	3.110	18.7	0.043	0.26	280
k_d = 0.04 day^{-1}	250	3.326	14.4	0.050	0.38	104
μ_s = 9.0 day^{-1}	125	1.786	7.5	0.100	0.40	123
	63	0.634	2.7	0.120	0.40	79
Graded bed #3	500	3.701	16.0	0.043	0.39	158
k_d = 0.04 day^{-1}	250	2.736	12.0	0.086	0.39	100
μ_s = 6.0 day^{-1}	125	1.390	6.0	0.100	0.39	121
	63	0.734	3.2	0.110	0.39	86

[a] Low effective porosity believed to be the result of dead volume in column.

approximately three pore volumes, incorporating over 99% of the mass recovered. Nonetheless, despite the fact that adsorption alone could reproduce the curve peak that incorporates most of the mass of phages recovered during the experiment, first-order deposition alone was incapable of reproducing the tailing observed. A desorption term was thus necessary. Application of this term improved the correspondence between the observed and simulated curves in the tailing section. However, simple adsorption/desorption alone could not reproduce the sloping tail observed in T7s breakthrough curves following the point of inflection. This gentle sloping phenomenon is attributed to viral inactivation (Schijven et al., 1999). Since source reservoir concentrations indicated that the rate of T7 inactivation in the liquid was not significant over the duration of any of the experiments, T7 inactivation on the column matrix was concluded to be responsible for the gradual decline in the concentration in desorbing bacteriophage. In order to simulate this phenomenon, the rate of desorption was increased and a concomitant inactivation rate on the surface applied using the model. The results of these simulations are also presented in Fig. 5.

4.3. Natural gravels—granulometry and transport simulations

The results of granulometric analyses, such as those presented in Fig. 3, have been used to ascertain the hydraulic conductivity variation with depth in the FU sequence sampled at

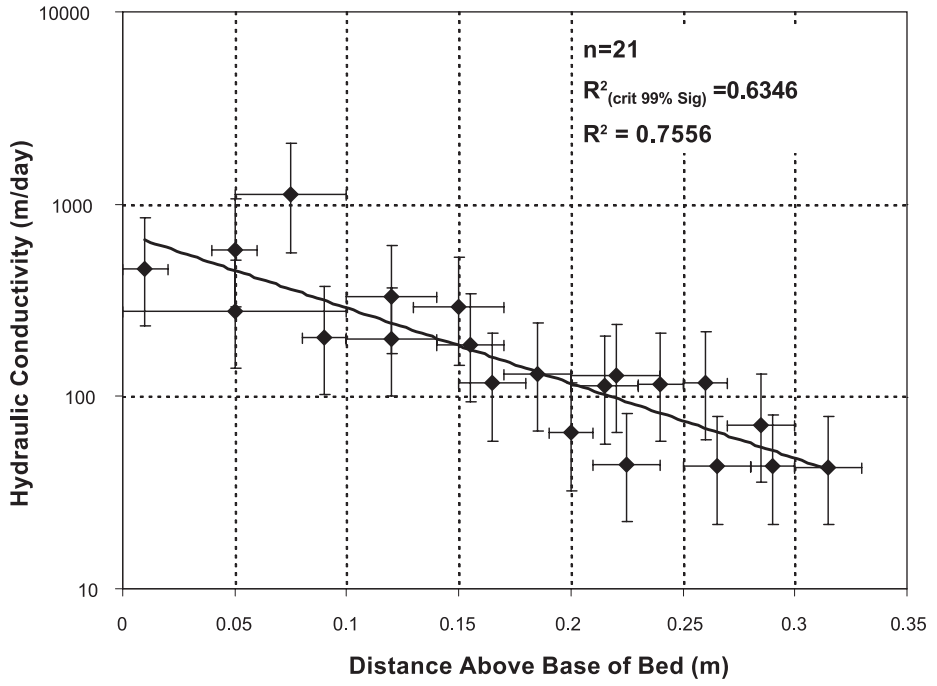

Fig. 6. Plot of calculated hydraulic conductivity with distance from base, fining-upwards sequence in Walperswil gravel. Inlay values: Critical and observed r^2 values. Note: Hydraulic conductivity errors calculated based on plus or minus 5% porosity variation.

Walperswil. Fig. 6 presents the results of the hydraulic conductivity calculations based on these granulometric analyses. The data show a statistically significant log-linear variation in hydraulic conductivity from the base to the bed to the top, with values at the top of the bed being approximately an order of magnitude lower than those found at the base. For the 50-cm-thick bed under consideration in the simulations, hydraulic conductivity was assumed to vary by a similar magnitude between the base and the top of the simulated FU sequence. The parameters used in these simulations are presented in Table 3.

Fig. 7A and B presents the results of solute and bacteriophage transport simulations in the FU sequence for both coarse-grained and fine-grained beds assuming equal flow velocities. It is noteworthy that although the solute profiles for both beds are equal, phage peak concentrations and resulting recoveries are significantly lower in the finer-grained unit. This occurs despite equivalent groundwater flow velocities, as reflected by identical conservative tracer breakthrough curves. Moreover, a significant difference in peak concentration times is apparent between conservative and bacteriophage tracers in the latter case (Fig. 7B). Furthermore, the relative contributions of each subunit, in both coarse-grained and fine-grained sequences, are presented in Table 3 and demon-

Table 3
Model inputs and relative proportions of solute and phage recovery for solute and phage transport simulations in fining-upward sequence

Grain diameter (μm)	Advective velocity (m day^{-1})	Dispersion coefficient (m^2 day^{-1})	Proportion of solute recovery (%)	Proportion of phage recovery (%)	k_c (day^{-1}) ($\alpha = 0.3$)	k_d (day^{-1})	μ_s (day^{-1})
Coarse-grained fining-upwards sequence $\alpha = 0.3$							
10,000	34.6	0.432	44.0	68.0	21	0.003	3.0
7499	19.4	0.243	24.8	25.7	27	0.003	3.0
5623	10.9	0.137	13.9	5.8	37	0.003	3.0
4217	6.1	0.077	7.8	0.4	49	0.003	3.0
3162	3.5	0.043	4.4	<0.1	65	0.003	3.0
2317	1.9	0.024	2.5	<0.1	87	0.003	3.0
1778	1.1	0.014	1.4	<0.1	116	0.003	3.0
1334	0.6	0.008	0.8	<0.1	154	0.003	3.0
Peak solute conc: 39% at 0.37 pore volumes (PV). Peak phage conc: 32% at 0.37 PV							
Averaged value simulation							
4498	9.8	0.122	100.0	1.0	38.7	0.003	3.0
Peak solute conc: 31% at 1.0 pore volumes. Peak phage conc: 0.5% at 0.96 PV.							
Fine-grained fining-upwards sequence $\alpha = 0.1$							
1000	34.6	0.432	44.0	99.5	318	0.03	3.0
750	19.4	0.243	24.8	0.5	425	0.03	3.0
562	10.9	0.137	13.9	<0.1	566	0.03	3.0
422	6.1	0.077	7.8	<0.1	755	0.03	3.0
316	3.5	0.043	4.4	<0.1	467	0.03	3.0
237	1.9	0.024	2.5	<0.1	1342	0.03	3.0
178	1.1	0.014	1.4	<0.1	1790	0.03	3.0
133	0.6	0.008	0.8	<0.1	2387	0.03	3.0
Peak solute conc: 39% at 0.37 pore volumes. Peak phage conc: 0.7% at 0.33 PV.							

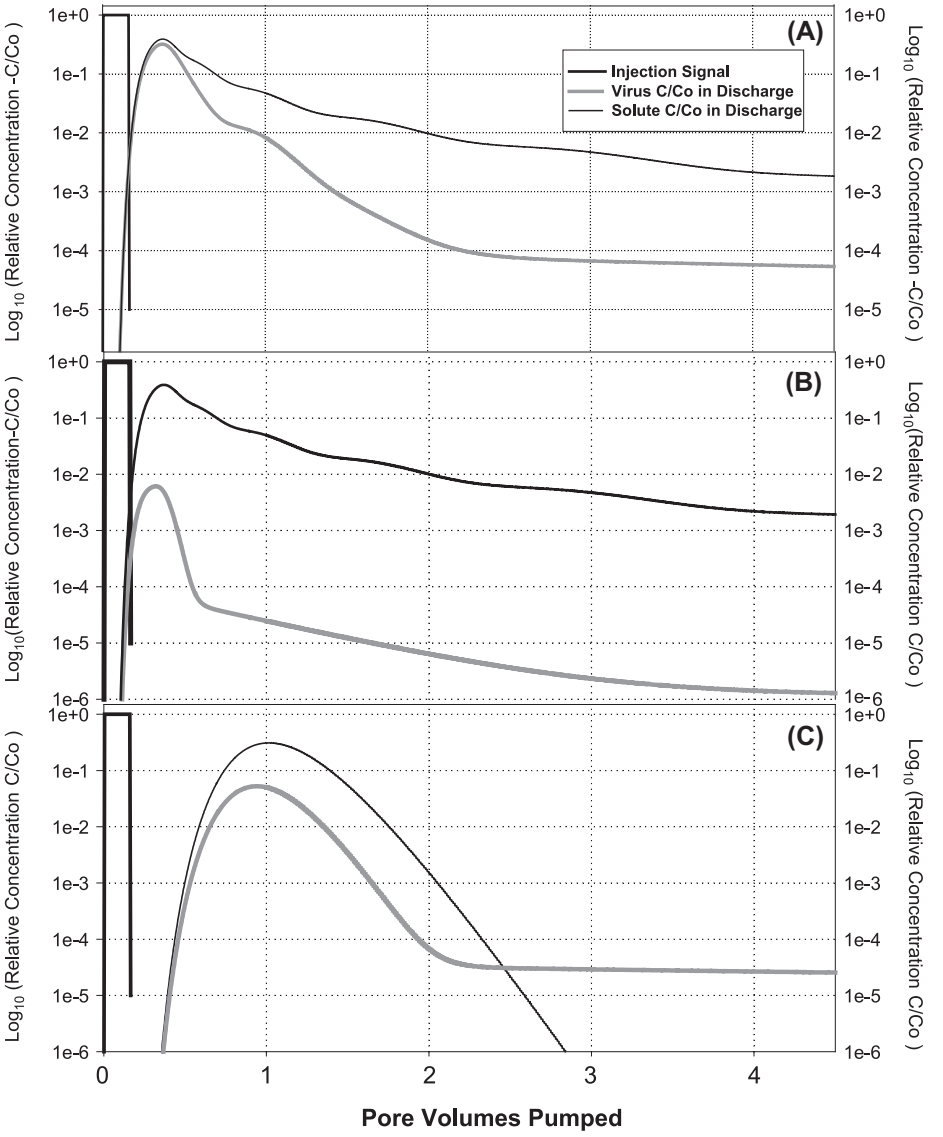

Fig. 7. Results of analytical simulations of solute and virus transport in graded beds. (A) Bed grain size 10000 μm at base, 1000 μm at top.; $\alpha = 0.3$. (B) Bed grain size 1000 μm at base, 100 μm at top; $\alpha = 0.1$. (C) Simulation for coarse-grained bed, assuming averaged grain diameter (4498 μm). $\alpha = 0.1$. Note peak virus concentrations are significantly lower than heterogeneous system with sedimentary structure, despite lower collision efficiency. Tracer first arrival and peak arrival times are also later.

strate that a much greater relative contribution to total recovery is made by bacteriophage in the coarsest bed of the fine-gained sequence, relative to that in the coarser-grained unit.

Fig. 7C and Table 3 also present the results of solute and bacteriophage simulations assuming averaged hydraulic conductivity and grain size for the coarse-grained bed. Peak solute and phage concentrations in the discretised heterogeneous beds and the averaged simulation differ significantly. The averaged systems peak arrival time is significantly later than that of the heterogeneous system. Moreover, phage peak concentrations are significantly lower in the averaged system. Furthermore, additional simulations have shown that the difference between averaged and discretised simulations increases with increasing hydraulic conductivity contrast between the base and top of the bed.

5. Discussion

The results of the experiments carried out using uniformly sized beads demonstrate that all bead sizes have a significant capacity to attenuate T7 under ambient experimental conditions. Moreover, the similarity of values for the collision efficiencies, determined at different flow rates using the uniform column test data, suggests that Tien and Payatakes (1979) approach to calculating deposition constants is appropriate for phage filtration. This approach has allowed deposition constants for T7 to be determined for the various layers in the graded column experiments using advective velocity data derived from fluorescein breakthrough curves. These deposition constants have successfully permitted T7 concentration peak responses in all graded column experiments to be simulated, since potentially important terms, such as viral inactivation do not play a significant role in influencing the maximum concentrations observed. However, additional terms simulating desorption and viral inactivation on bead surfaces needed to be incorporated to account for the tailing after the T7 peak had passed. Since bacteriophage inactivation in liquid was negligible throughout all experiments and the results of the experiments show that significant inactivation is occurring while T7 is adsorbed, the beads are thus believed to accelerate inactivation of T7. The reader is referred to Grant et al. (1993) for further details on possible inactivation mechanisms associated with this process.

Experimental solute and bacteriophage breakthrough curves bear a strong resemblance to breakthrough curves previously observed in field-based tracer testing in porous media (Kennedy et al., 2001a,b; Woessner et al., 1998). As previously noted, analysis of these curves using conventional mass transport solutions is unable to reproduce the breakthrough curves observed with single advective velocity and dispersion coefficient terms. This suggests that the distribution of hydraulic conductivities in many aquifers is more complex than often assumed and needs to be accounted for by phenomena such as the internal structure of individual beds.

The results of grain-size analyses of the sand and gravel samples collected from the bed containing the FU sequence at the Walperswil gravel pit indicate a strong log-linear variation in hydraulic conductivity with distance from the base of the bed. Flow and transport processes in this structure were modelled using a series texturally uniform subunits with the same overall degree of grain size/hydraulic conductivity variation as that observed in the FU sequence sampled in the field. Resulting conservative tracer breakthrough curves generated by superimposing a series of flux-weighted advective–dispersive terms bear a strong resemblance to solute breakthrough curves observed in

tracer tests completed at the nearby Kappelen test site (Fig. 1), and other porous media/ fractured rock test sites (Kennedy, 2000). Moreover, by applying a uniform collision efficiency to the discretised structure, the dependency of bacteriophage breakthrough on grain size, and thus, deposition constant could be evaluated. Once again responses bear a strong qualitative resemblance to those observed at the Kappelen field site and other porous media sites (e.g. Kennedy et al., 2001a,b; Woessner et al., 1998) where bacteriophage maximum concentrations occurred before those of solutes and bacteriophage recovery is significantly lower than that of the dissolved tracer.

Despite the similarities between simulated and observed results, it is important to recognise that the responses must be regarded as simplifications of virus transport in natural systems. This arises largely from the fact that collision efficiency is unlikely to be uniform in natural deposits, but will depend strongly upon the chemical nature of the aquifer matrix (mineralogy) (Schijven et al., 2000). Mineralogy may vary within individual beds and is dictated by parameters such as the energy of the transporting medium at the time of deposition, grain dimensions and mineral density (Allen, 1985). Consequently, minerals such as clays will be more likely deposited at the end of depositional events when available energy is waning and conditions for settling of finer-grained material are more favourable. Investigations by Rossi and Aragno (1999) demonstrated that clay minerals such as montmorillonite and attapulgite can have significant phage attenuation capacity. Moreover, these fine-grained minerals can also influence the hydraulic conductivity of the sediments thereby controlling the groundwater velocity, and by inference, the residence time of water in the system. Furthermore, greater residence time increases the possibility of adsorption of phage to mineral surfaces. Consequently, complex phage breakthrough curves can be generated in compositionally and/or texturally heterogeneous aquifers even over small distances.

On a larger scale, the spatial distribution of a sedimentary structure will depend upon its depositional environment. Indeed identification of an appropriate sedimentary facies model can assist considerably in evaluating the suspected extent of a particular sedimentary unit/structure, and thus the resulting form of tracer/contaminant plumes. For example, contaminants in a gravel-rich channel fill deposit are likely to have a different distribution to that in an equivalent sized material deposited as a sheet of sand and gravel.

Overall, the results of the simulations highlight the importance of geological conditions in predicting bacteriophage transport in porous aquifers. Both the distribution of grain size and the collision efficiency of the bacteriophage with the grains strongly determine the degree of attenuation in heterogeneous deposits, such as those containing FU sedimentary structures. Indeed, if predictions concerning solute and bacteriophage mass transport are simplified, and uniform conditions assumed, such as were simulated for the coarse-grained FU sequence, the resulting predictions will underestimate the maximum concentration of bacteriophage observed. Furthermore, the total mass of bacteriophage anticipated at a monitoring point will be under-estimated.

The results of this study demonstrate the importance of geological heterogeneity in site characterisation when considering viral transport in groundwater, particularly with respect to grain size and mineralogy. In a more general sense, the data and associated simulations further underscore the importance of appropriate site characterisation techniques when considering protection of groundwater as a drinking water supply.

Acknowledgements

This research was funded by the Swiss National Science Foundation (Grant Number: FN-20-061370.00). The authors wish to express their thanks to Mrs. Magali Grob for carrying out the bacteriophage analyses, Potters Industries, Germany for supplying the glass beads, and Mr. Hurni of Kies und Betonwerke, Sutz, for access to Walperswil quarry.

References

Allen, J.R.L., 1985. Principles of Physical Sedimentology, First edition. Allen & Unwin, Herts, p. 272.

Bales, R.C, Shimin, L., Maguire, K.M., Yahya, M.T., Gerba, C.P., Harvey, C., 1995. Virus and bacteria transport in a sandy aquifer, Cape Cod, MA. Groundwater 33 (4), 653–661.

Bear, J., 1972. Dynamics of Fluids in Porous Media. Elsevier, New York, p. 764.

Bolster, C.H., Mills, A.L., Hornberger, G.M., Herman, J.S., 1999. Spatial distribution of deposited bacteria following miscible displacement experiments in intact cores. Water Resour. Res. 35 (6), 1797–1807.

De Hoog, F.R., Knight, J.H., Stokes, A.N., 1982. An improved method for numerical inversion of Laplace transforms. SIAM J. Sci. Statist. Comput. 3, 357–366.

Dieulin, A., 1980. Pollutant propagation in an alluvial aquifer: the effect of flow paths. pp. 207. PhD thesis. Pierre and Marie Curie University, Paris VI.

Freeze, R.A., Cherry, J.A., 1979. Groundwater, First edition. Prentice-Hall, New York, p. 604.

Grant, S.B., List, E.J., Linsstom, M.E., 1993. Kinetic analysis of virus adsorption and inactivation in batch experiments. Water Resour. Res. 29, 2067–2085.

Harter, T., Wagner, S., Atwill, E.R., 2000. Colloid transport and filtration of *Cryptosporidium parvum* in sandy soils and aquifer sediments. Environ. Sci. Technol. 34 (1), 62–70.

Harvey, R.W., Garabedian, S., 1991. Use of colloid filtration theory in modeling movement of bacteria through a contaminated sandy aquifer. Environ. Sci. Technol. 25 (1), 178–185.

Johnson, P.R., Ning, S., Elimelech, M., 1996. Colloid transport in geochemically heterogenous porous media: modeling and measurements. Environ. Sci. Technol. 30, 3284–3293.

Kass, W., 1997. Tracing Technique in Geohydrology, First edition. A.A. Balkema, Rotterdam, p. 581.

Kennedy, K., 2000. Bacteriophages as particle migration indicators in subsurface environments. Tracers and modelling in hydrogeology. IAHS Publ. 262, 151–158.

Kennedy, K., Muller, I., Schnegg, P., Rossi, P., Koezel, R., 2001a. Characterisation of the Kappelen Groundwater Research Site (BE), Switzerland and preliminary bacteriophage and solute tracer component responses. Beitr. Hydrogeol. 52, 158–180.

Kennedy, K., Niehren, S., Rossi, P., Schnegg, P.A., Müller, I., Kinzelbach, W., 2001b. Results of bacteriophage, microsphere and solute tracer migration comparison at Wilerwald Test Field, Switzerland. Beitr. Hydrogeol. 52, 180–210.

Kretzschmar, R., Barmettler, K., Grolimund, D., Yao-de, Y., Borkovec, M., Sticher, H., 1997. Experimental determination of colloid deposition rates and collision efficiencies in natural porous media. Water Resour. Res. 33 (5), 1129–1137.

Kretzschmar, R., Borkovec, M., Grolimund, D., Elimelech, M., 1999. Mobile subsurface colloids and their role in contaminant transportAdvances in Agronomy, vol. 66. Academic Press, San Diego, pp. 121–193.

Lawrence, J.R., Hendry, M.J., 1996. Transport of Bacteria through geologic media. Can. J. Microbiol. 42, 410–422.

Macler, B., Merkle, J.C., 2000. Current knowledge on groundwater microbial pathogens and their control. Hydrogeol. J. 8, 29–40.

Maloszewski, P., 1992. Mathematical modelling of tracer transport in different aquifers: results from ATH test fields. In: Hoetzl, H., Werner, A. (Eds.), Proc. 6th Int. Symp. Water Tracing, Karlsruhe. A.A Balkema, Rotterdam, pp. 25–30.

Martin, R.E., Bower, E.J., Hanna, L.M., 1992. Application of clean bed filtration theory to bacterial deposition in porous media. Environ. Sci. Technol. 26, 1053–1058.

Martin, M.J., Logan, B.E., Johnson, W.P., Jewett, D.G., Arnold, R.G., 1996. Scaling bacterial filtration rates in different sized porous media. Environ. Eng., 407–415 (May).

Moore, R.S., Taylor, D.H., Reddy, M.M.M., Sturman, L.S., 1982. Adsorbtion of reovirus by minerals and soils. Appl. Environ. Microbiol. 44, 852–859.

Penrod, S.L., Olsen, T.M., Grant, S.B., 1996. Deposition kinetics of two viruses in packed beds of quartz granular media. Langmuir 12, 5576–5587.

Rajagopalan, R., Tien, C., 1976. Trajectory analysis of deep-bed filtration with the sphere-in-a-cell porous media model. AIChE J. 28, 523–533.

Reading, H.G., 1986. Sedimentary Facies and Environments, Second edition. Blackwell, Oxford, p. 615.

Redman, J.A., Estes, M.K., Grant, S.B., 2001. Resolving macroscale and microscale heterogeneity in virus filtration. Colloids Surf., A Physicochem. Eng. Asp. 191 (1–2), 57–70.

Robertson, J.B., Edberg, S.C., 1997. Natural protection of spring and well drinking water against surface microbial contamination: 1. Hydrogeological parameters. Crit. Rev. Microbiol. 23 (2), 143–178.

Rossi, P., Aragno, M., 1999. Analysis of bacteriophage inactivation and its attenuation by adsorption onto colloidal particles by batch agitation techniques. Can. J. Microbiol. 45, 9–17.

Rossi, P., Kass, W., 1997. Phages. In: Kass, W. (Ed.), Tracing Technique in Geohydrology, First edition. A.A. Balkema, Rotterdam, pp. 244–271. Section 2.8.

Saiers, J.E., Hornberger, G.M., 1996. The role of colloidal kaolinite in the transport of cesium through laboratory sand columns. Water Resour. Res. 32 (1), 33–41.

Schijven, J.F., Hoogenboezem, W., Hassanizadeh, S., 1999. Modelling removal of bacteriophages MS-2 and PRD-1 by dune recharge at Castricum, Netherlands. Water Resour. Res. 35 (4), 1101–1111.

Schijven, J.F., Medema, G.J., Vogelaar, A.J., Hassanizadeh, S.M., 2000. Removal of bacteriophages MS-2 and PRD-1, spores of *Clostridium bifermentans* and *E. coli* by deep well injection. J. Contam. Hydrol. 44, 301–327.

Schijven, J.F., Hassanizadeh, S., de Bruin, H.A.M., 2002. Column experiments to study nonlinear removal of bacteriophages by passage through saturated dune sand. J. Contam. Hydrol. 58 (3–4), 243–259.

Schnegg, P., Bossy, F., 2001. Sonde for downhole measurement of water turbidity and dye tracer concentration. In: Seiler, K.P., Wohnlich, S. (Eds.), New Approaches Characterizing Groundwater Flow, vol. 2. Swets and Zeitlinger, Lisse, pp. 795–799.

Silliman, S.E., 2000. Particle transport through two-dimensional, saturated porous media: influence of physical structure of the medium. J. Hydrol. 167, 79–98.

Tien, C., Payatakes, J., 1979. Advances in deep bed filtration. AIChE J. 25, 737–759.

van der Leeden, F., Troise, F.L., Todd, D.K., 1990. The Water Encyclopedia, First edition. Lewis, Chelsea, MI, p. 808.

Woessner, W., DeBorde, D., Haigh, M.J., Kreck, J., Rajwar, G.S., Kilmartin, M.P., 1998. Virus transport in the floodplain of a headwater stream, western Montana, USA. Headwaters: Water Resources and Soil Conservation, First edition. A.A. Balkema, Rotterdam, pp. 197–207.

Yao, K.M., Habibian, M.T., O'Melia, C.R., 1971. Water and waste water filtration: concepts and applications. Environ. Sci. technol. 5, 1105–1112.